

Paper Submitted to the  
1964 Dubna Conference  
on High Energy Physics.

NPA/INT 64-25  
Meyrin, 3rd August, 1964.

PROGRESS REPORT ON EXPERIMENTAL STUDY OF NEUTRINO INTERACTIONS IN THE  
CERN H.L.B.C.

M.M. Block, H. Burmeister, D.C. Cundy, B. Eiben, C. Franzinetti, J. Keren,  
R. Møllerud, G. Myatt, A. Orkin-Lecourtois, M. Paty, D. Perkins, C.A. Rams,  
K. Schultze, H. Sletten, K. Soop, R. Stump, W. Venus, H. Yoshiki.

Introduction

The analysis of the experimental data from the 1963/64 runs of the HLBC is still in progress. This paper reports some of the new analysis since Sienna<sup>(1)</sup>, and reviews the status of some of the conclusions presented then.

Since the Sienna Conference the inner conductor of the neutrino horn has been modified, with the result that the expected neutrino spectrum was significantly greater at high energies.

Most of the problems considered here have been already mentioned in our previous paper<sup>(1)</sup> and can be discussed now on the basis of our larger statistics. The present report is only a preliminary note summarising our results up to date.

Event Rate

During 1963 and 1964, the neutrino experiment at CERN has used  $1.054 \times 10^6$  machine pulses from the PS, with a total integrated extracted beam of  $7.3 \times 10^{17}$  protons on the copper target of the horn. About 800 events attributable to  $\nu_{\mu}$  interactions have been found in the 500 litres of  $\text{CF}_3\text{Br}$  filling the heavy liquid bubble chamber. This analysis refers to 454 events contained in a fiducial volume of 220 litres, defined to obtain good track measurability and  $\gamma$  - ray conversions.

In each of the 454 events there is at least one negative lepton candidate, together with other particles. There are 236 non-pionic events, containing only a  $\mu^-$  candidate and nucleons, and 218 mesonic events. Forty events have one or more fast positive particles which cannot be identified. However, an analysis of pions identified by  $\delta$  - rays indicates that only about four of these unidentified particles are pions. In subsequent analysis all unidentified fast particles are assumed to be protons. Figure 1 gives the detailed pionic event classification. A total of 9 events with strange particles is not included in the Fig. 1.

Seven events with one identified negative electron have been found; two of these events have in addition a  $\mu^-$  candidate. One previously reported event having a positron and  $\mu^-$  candidate has been found.

#### The $\nu^-$ spectrum

The spectrum has been calculated by S. van der Meer using experimental pion and kaon production data from counter experiments<sup>(2)</sup>.

A direct measurement of the pion spectrum emitted from a copper target identical with that of the neutrino horn, has been carried out using the Ecole Polytechnique Heavy Liquid Bubble Chamber and is still in progress.

Preliminary results for neutrinos and anti-neutrinos between 0.1 and 2 Gev suggest that the intensity below 1 Gev is 50 o/o greater than previous predictions (see Fig. 6).

#### Intermediate Boson

The intermediate vector-boson is expected to decay predominantly in the following modes.

$$\begin{aligned} W &\rightarrow \mu + \\ &\rightarrow e + \\ &\rightarrow n \pi's, K's \end{aligned}$$

The two leptonic modes are assumed to leave the same decay probability. The non-leptonic branching ratio is not known.

This experiment cannot detect the  $\mu\nu$ -mode. We have seen one "candidate" for the positron decay out of 454 events in the fiducial volume. We expect about .5 positron events from  $\bar{\nu}_e$  background.

If the mass of the boson were 1.8 Gev, we would expect 3 events of  $W^-$  production. Thus the result indicates a lower limit of 1.8 Gev/c for  $M_W$ , unless the pionic mode were predominant.

For the pionic mode we have restricted the analysis to events with  $E_{vis} \geq 6$  Gev : we expect in fact that if the  $W$  exists, its production would tend to predominate over other inelastic processes with increasing energy.

We have observed 23 events above 6 Gev. Of these only 14 have a total mesonic charge of +1, as required if the  $W^-$  production is elastic. No obvious peak is observed in the effective pion mass distribution. (Fig. 2)

On the basis of event rate a mass of 1 Gev is excluded, but there are 8 events in the region 1 to 2 Gev where 11 are expected if  $M_W = 1.5$  Gev, therefore this value for the mass cannot be excluded. The error in the effective mass is large in these events due to the high multiplicity (on average  $> 5$ ). The analysis is further complicated by short charged tracks and the possibility of missing  $\gamma$  - rays or neutral particles (the  $\gamma$  - ray detection efficiency is 0.84; two events have a  $K^0$ ).

Thus we have no clear evidence for the existence of the intermediate boson. We therefore conclude that its mass is greater than 1.5 Gev and if the leptonic decay predominates, its mass cannot be less than 1.8 Gev.

### Elastic Events and Form Factors

The non-pionic events, from which the elastic events must be extracted, contain three types of background :

1. Neutron stars in which a non-interacting  $\pi^-$  is misidentified as a  $\mu^-$ .
2. Interacting incoming particles (usually  $\pi^+$ ) which are misidentified as outgoing particles of opposite charge.
3. Pionic neutrino events in which the pions have been absorbed in the parent nucleus.

The unidentifiable background due to processes 1 and 2 is estimated from the number of similar events which have been identified by scattering, interactions,  $\delta$  - rays, etc. Most of these events are of low energy and we estimate that above 1 Gev, only one event from these types of background is present in the sample of non-pionic events.

The pionic absorption was estimated by considering the number of observed single pion events and the pion absorption cross-section. For this correction, we assumed that all pions are produced in the process



For each event a pion distribution in the lab system was derived from the  $\mu$  - momentum and angle assuming that the angular distribution of the pion in the centre of the mass system of the  $N^*$  is isotropic. From pion absorption data<sup>(3)</sup>, the probability of absorption of pions of the calculated energy spectrum was determined. The number of absorbed pions produced in 1  $\pi$  - events has thus been estimated to be 40.

The analysis of elastic events and the estimation of the form factors involved was carried out essentially on the basis of the 4-momentum transfer distribution. The  $q^2$ 's were derived from the  $\mu$  -energy and angle, and assuming the event to be elastic and the target nucleon to be at rest.

Using the method discussed above the observed distribution was corrected for the background of  $1 \pi$  events which appeared as non-pionic.

For the determination of the axial vector form factor we have considered only events with total visible energy ( $E_{\text{vis}}$ ) greater than 1 Gev, since below this energy the  $q^2$  distribution is determined largely by kinematical effects, which are independent of the form factors.

Figure 3 shows the corrected  $q^2$  distribution of these events and that of the calculated background. The curve represents the expected distribution with an axial vector form factor taken to be  $(1 + (q/1.3)^2)^{-2}$ . Neglecting the induced pseudoscalar term and the muon mass, the cross-section  $\frac{d\sigma}{dq^2}$  is given by

$$\frac{d\sigma}{dq^2} = \frac{q^2}{32 \pi E_\nu^2} \left[ A + B(4ME_\nu - q^2) + C(4ME_\nu - q^2)^2 \right]$$

$$\text{where } A = q^2 \left( 4F_A^2 \lambda^2 - 4F_1^2 \right) + q^2 \left( F_1^2 + \mu^2 \frac{F_2^2}{M^2} + \frac{4\mu F_1 F_2}{M} + \lambda^2 F_A^2 \right) - q^2 \frac{\mu^2 F_2^2}{4M^2}$$

$$B = 4q^2 \left( F_1 + \frac{\mu F_2}{M} \right) \lambda F_A$$

$$C = F_1^2 + \lambda^2 F_A^2 + q^2 \frac{\mu^2 F_2^2}{4M^2}$$

and

$E_\nu$  = neutrino energy

$M$  = protonic mass

$\lambda = \frac{G_A}{G} = 1.15$

$\mu = \mu_p - \mu_n = 3.79$  Bohr nucleon magneton

$F_1, F_2$  = vector form factors

$F_A$  = axial vector form factors

} normalised to 1 for  $q^2 \rightarrow 0$

A form factor analysis is presented here, which is independent of the neutrino spectrum. The observed  $q^2$  distribution  $\frac{dN}{dq^2}$  is given by

$$\frac{dN}{dq^2} = c \int \phi(E) \frac{d\sigma(E)}{dq^2} dE$$

when  $\phi(E)$  is the neutrino flux at energy E.

$$\begin{aligned} \text{as } c \phi(E) &= \frac{1}{\sigma(E)} \frac{dN}{dE} \\ \frac{dN}{dq^2} &= \int dN \frac{1}{\sigma(E)} \frac{d\sigma(E)}{dq^2} \\ &= \sum \frac{N(E)}{\sigma(E)} \frac{d\sigma(E)}{dq^2} \end{aligned}$$

where  $N(E)$  is the number of events in the energy interval  $E$  to  $E + \Delta E$ .  
 $\sigma(E)$  and  $\frac{d\sigma(E)}{dq^2}$  are calculable if the axial vector form factor is known.

This theory has to be corrected for effects of Fermi momentum and Exclusion Principle when the interaction takes place in complex nuclei. Both effects have been calculated<sup>(4)</sup> using a Fermi gas model of momentum distribution of the nucleus with a maximum momentum of 267 Mev/c. The effect of this model is to reduce the cross-section at low  $q^2$ . For  $M_A = M_v$  we estimate the following reductions.

$q^2$ (Gev/c) <sup>2</sup>	o/o Reduction
0 to .1	48
.1 to .2	16
.2 to .3	3
.3 to .4	0

The model also indicates that above  $q^2 = .3$  the true  $q^2$  of the event and that calculated assuming the target neutron to be at rest, i.e.  $q^2_{\text{calc}}$  have identical distributions.

A maximum likelihood method was used to obtain the best fit for  $M_A$ . The result is shown in Fig. 4. It is to be noticed that if  $M_A = M_v$ , then  $M_A = 0$  will also be a good fit. However, this zero solution can be excluded both from  $\mu$ -capture data and the neutrino event rate in the region 1 - 2 Gev where the spectrum is known to 30 o/o.

The best fits for the various vector form factors can be tabulated as follows :

	$F_V$	$F_A$	$M_A$
Older formulation	$(1 + (q/0.84)^2)^{-2}$	$(1 + q^2/M_A^2)^{-2}$	1.05 + 0.35 - 0.20
"Stanford" form factors	$1.19 (1 + (q/0.6)^2)^{-2}$ - 0.19	$(1 + q^2/M_A^2)^{-2}$	1.0 + 0.25 - 0.25
	$1.19 (1 + (q/0.6)^2)^{-2}$ - 0.19	$(1 + q^2/M_A^2)^{-1}$	0.6 + 0.2 - 0.6

The errors quoted above are statistical whereas the true error is also determined by the accuracy of the background estimate.

Since the form factor calculation depends critically on the background estimate, an independent check is desirable. For this purpose all non-pionic events have been subjected to a kinematic test. It is assumed that the event is elastic, and has taken place on a neutron at rest. This allows one to calculate  $E_V$ : Assuming that the maximum Fermi momentum is 267 Mev/c, one can calculate the maximum possible disturbance to the available energy. If  $E_{vis}$  is greater than the maximum calculated energy by more than two standard deviations, the event is classed as inelastic. Since the method is only sensitive at low  $q^2$  it does not give a complete check of the background calculation. However, 8 events with  $q^2 < 0.2$  have been identified as inelastic by the test. The background calculation, as described earlier, predicts 9 events in the same  $q^2$  range. Since the kinematic test will not identify all the inelastic events even at low  $q^2$ , it must be concluded that the background correction is, if anything, underestimated.

If the background is doubled, the best value of  $M_A$  becomes  $1.38 \pm 0.36$ . Thus considering both statistical and systematic errors, we may give a value  $M_A = 1.0 \pm 0.5$ .

The fits obtained are good, the  $\chi^2$  being 3.3 for 10 degrees of freedom suggests that the mass parametric representation of the axial-vector form factor is a good approximation.

However, one can extract  $F_A$  directly from the data if one knows the absolute flux in the experiment. It is a good approximation to consider  $F_A = F_V$  in the region of  $0 < q^2 < 0.2$  (Gev/c)<sup>2</sup>. Thus from the observed number of events in this  $q^2$  limit it is possible to calculate the effective flux, which then can be used to extract  $F_A$  at higher  $q^2$ . Figure 5 shows the results of this analysis in terms of  $F_A/F_V$ .

From the elastic cross-section calculated using the "best fit" value of  $M_A$ , values of the neutrino flux,  $\phi_\nu$ , at various energies, up to 5 Gev, can be derived. The experimental points for  $\phi_\nu$  ( $E_\nu$ ) thus obtained are displayed in Fig. 6. They are seen to be consistent with the values which have been calculated on the basis of the measured spectra of  $\pi$ 's and K's (full line) except at low neutrino energy. The dotted line indicates a correction introduced by the latest results obtained from the HLBC experiment referred to in section 2.

### Single $\pi$ production

Single  $\pi$  production is expected to take place mainly via the  $(\frac{3}{2}, \frac{3}{2})$  isobar; other processes such as the "peripheral"  $1\pi$  or  $\omega^0$  exchange may play a minor role, their cross-section having been calculated to be of one or two orders of magnitude smaller.

$N^\pi$  production implies a ratio of final states

$$p\pi^+ : p\pi : n\pi^+ = 9 : 2 : 1 \quad (1)$$

which means an overall ratio  $\pi^+/\pi^0 = 5/1$ .



The observed ratio for all  $1\pi$  events is 79/41 or  $\sim 2$ . The detailed ratios have been computed on  $(1\pi, 1p)$  and  $(1\pi, 0p)$  events only and it has been found to be 42 : 17 : 14.

The charge distribution is distorted by interaction of the final products in the nucleus. Charge exchange processes certainly play a large role as indicated by the presence of  $\pi^-$  in single pion events.

Therefore little can be said about the  $N^*$  production by this method except that the observed ratios are compatible with a large fraction of the  $1\pi$  events being due to  $N^*$ . Alternatively one may look for  $N^*$  production by observing the mass of the recoiling system in the process

$$\nu + N \rightarrow \mu^- + N^*$$

$$M^{*2} = M^2 - q^2 + 2M(E_{\text{vis}} - E_{\mu})$$

where  $M$  = Nucleon mass,  $E_{\nu}$  is taken to be the visible energy of the event. This  $M^*$  distribution is broadened by Fermi motion and distorted to low values by energy loss of the  $\pi$  and nucleon in nuclei. Figure 7 shows a plot of  $M^*$  versus  $E_{\text{vis}}$  for all pionic events.

At low energy, a "phase space" distribution of the final products would yield mass values grouped around the value of the isobar mass, for kinematical reasons. Therefore we consider events of visible energy larger than 1.5 Gev at which the phase space distribution would differ considerably from that due to the isobar. Figure 8 shows a histogram of  $M^*$  for single  $\pi$  events with  $E_{\text{vis}} \geq 1.5$  Gev, and is considered good evidence for some fraction of  $N^*$  production. A prominent peak is seen, for  $M^* = 1.2$  Gev. About 30 o/o of the events lie outside the peak and must be attributed to other processes. It may be worth noting that the majority of them are associated with fast protons which would not be expected if these events were due to "peripheral"  $1\pi$  exchange.

If one makes the assumption of exclusive  $N^*$  production then a cut-off at  $M^* = 1.4$  Gev will certainly contain most of the sample. Figure 9 shows the  $\pi$  cross-section using this criterion. The data have been corrected for pion absorption in both the 1 and 2 pion events. As can be seen the theoretical cross-section calculated using form factors  $F_A = F_V = (1 + (q/0.9)^2)^{-2}$

is too high by a factor of 2. On the other hand the cross-section for one pion events in the range  $0 < q^2 < 0.2 \left(\frac{\text{Gev}}{c}\right)^2$  and  $1.0 < E_{\text{vis}} < 3.0 \text{ Gev}$ , after correction for absorbed pions, is :

$$\frac{d\sigma}{dq^2} = (0.5 \pm 0.2) \times 10^{-38} \text{ cm}^2 \left(\frac{\text{Gev}}{c}\right)^{-2}$$

in good agreement with the expected value of  $\sim 0.7 \times 10^{-38} \text{ cm}^2 \left(\frac{\text{Gev}}{c}\right)^{-2}$  per nucleon. The cross-section is based on the calculated spectrum and the effect of the exclusion principle (which is not expected to exceed 30 o/o) has been neglected.

#### Total inelastic cross-section

In the 1964 series of runs the neutrino flux above 8 Gev was increased, thus allowing a considerable improvement in the statistical accuracy of cross-sections at high energy. Figure 10 shows the observed energy distribution of all inelastic events. The total cross-section is also shown. The rise of  $\sigma_{\text{in}}$  with energy seems to be less pronounced than previously reported, although it is still uncertain due to poor statistics.

#### Strange particle production and $\Delta S/\Delta Q$ rule

If the  $\Delta S = \Delta Q$  rule were violated, events of the type

$$\nu + n = Y_1^{*+} + \mu^-$$

$$\nu + n = \Sigma^+ + \mu^-$$

could occur. If the  $\Delta S = \Delta Q$  rule were non-existent, consideration of  $SU_3$  symmetry would indicate an expected strange particle production of 5 o/o of the sum of elastic and  $\left(\frac{3}{2} - \frac{5}{2}\right)$  isobar production. The energy spectrum of the events would be similar to that of the elastic and isobar events.

In the energy range 1 - 4 Gev we have observed  $\sim 200$  events attributable to the elastic or to  $N^*$  production and in the same energy region only one event can possibly be interpreted as a single hyperon production, although associated production cannot be excluded. Considering the detection probability for hyperons, a violation of  $\Delta S = + \Delta Q$  of  $\sim 20$  o/o cannot be excluded. However, it should be noted that all the 9 events with strange particles, which extend up to energies of 11 Gev, are also compatible with associated production.

Other conclusions

In our previous report the following fundamental questions were discussed and conclusions reached. The data obtained with our latest run confirm those conclusions to a higher degree of accuracy. We shall limit ourselves to a brief summary of the results obtained up to now.

a)  $\nu_\mu \neq \nu_e$ . In fact, out of the 459 events which we have observed up to now, we have 5 events where the only negative track is an electron. All the electron energies are above 400 Mev. Assuming the same cross-section for  $\nu_e$  and  $\nu_\mu$ , we estimate that the  $\nu_e$  flux (from  $K_{e3}^+$  and  $K_{e3}^0$  decays) in the beam should give

1.1 elastic events;                    observed 2

2.2 inelastic events;                observed 3

b) The hypothesis that neutrinos coming from  $K_{\mu 2}^+$  decays could be  $\nu_e$  ( $K_{\mu 2}^+ \rightarrow \mu^+ + \nu_e$ ), often quoted as "neutrino flip hypothesis" predicts that with our  $\nu$ -spectra  $\sim 6$  o/o of all events observed in the chamber should be associated with  $e^-$  and no other lepton; this corresponds to 30 events. As our observed rate of  $e^-$  is .5 we conclude that the neutrino flip hypothesis is untenable.

c) Lepton conservation and neutral lepton currents. The limits on both neutral lepton currents and lepton non-conservation are set by the background of neutron stars. Since the runs of 1964 were made with higher neutrino flux at high energy, the neutron background from events in the shielding has increased. Therefore the best estimates on lepton conservation and neutral currents come from the 1963 runs, as previously reported. The limits are summarised below.

Leptonic conservation

Possible Process violating lepton conservation	Observed rate compared to total rate
$\nu_{\mu} + N \longrightarrow N + \pi$ at $E_{\nu} > 1 \text{ Gev}$	less than 2 o/o
$\nu_{\mu} + N \longrightarrow \mu^{+} + N$ at $E_{\nu} > 1 \text{ Gev}$	less than 6 o/o

Neutral currents

Possible Processes which may indicate the existence of lepton currents	Observed rate compared to elastic event rates
$\nu + p \longrightarrow \nu + p$	less than 3 o/o
$\nu + p \longrightarrow \nu + n + \pi^{+}$	less than 8 o/o

Acknowledgements

The neutrino experiment is especially indebted to Professors V.W. Weisskopf and G. Bernardini for their sustained enthusiasm, support and encouragement.

We have deeply appreciated the collaboration of J.S. Bell, H. Bingham, J. Løvseth, M. Nikolić and M. Veltman.

The observation of neutrino events in the heavy liquid bubble chamber was the culmination of technological development of many groups. It is with pleasure and gratitude that we acknowledge the construction and operation of the enhanced neutrino beam by M. Giesch, B. Kuiper, B. Langeseth, S. van der Meer, S. Pichler, G. Plass, G. Pluym, K. Vahlbruch, H. Wachsmuth and their colleagues; the operation and development of the heavy liquid bubble chamber by P. Innocenti and colleagues and the continued efforts to obtain the highest possible beam by the members of the Proton Synchrotron Division.

Finally, our warmest thanks to "the scanning girls" for their unstinted efforts and care with the data handling.

References

1. H.H. Bingham et al., Sienna Conference P-555 (1963).  
C.f. also J.S. Bell, J. Løvseth, M. Veltman, Sienna Conference P 587 (1963) for conclusions of the experiment comparison with theory, and reference to the literature.
2. D. Dekkers et al., NPA/Int 64-5 CERN internal report to be published in Phys. Rev.
3. Ronne et al., Arkiv För Fysik, 22, 193, (1962)  
Metropolis et al, Phys. Rev. 110, 204 (1958)  
Bruckner, Phys. Rev. 84, 262 (1951)
4. J. Løvseth, private communication.
5. G.R. Henry, J. Løvseth, J.D. Walecka, to be published.  
S. Berman and M. Veltman, private communication.

Figure captions

- Fig. 1 Inelastic event classification ( C = ambiguous positive track  
( $\pi, p$ ) el. rej. = non-pionic event found to be inelastic by  
kinematic test.)
- Fig. 2 Effective mass of pions in events where the total meson charge  
is + 1 and  $E_{\text{visible}} = 6$  Gev.
- Fig. 3 Final  $q^2$  distribution of non-pionic events and calculated background.
- Fig. 4 Log-likelihood as a function of  $M_A$  for elastic events.
- Fig. 5  $\frac{F_A}{F_V}$  as a function of  $q^2$ .
- Fig. 6 Neutrino flux calculated from event rate and cross-section  
compared with calculations based on properties of the neutrino  
horn.
- Fig. 7  $M^*$  as a function of neutrino energy ( $E_{\text{vis}}$ ) for all inelastic  
events.
- Fig. 8  $M^*$  distribution for single pion events with  $E_{\text{vis}}$  greater than  
1.5 Gev.
- Fig. 9 Energy distribution and cross-section of single pion events with  
 $M^*$  less than 1.4 Gev/c. Event rate corrected for pion absorption.
- Fig.10 Energy distribution and cross-section of all inelastic events.  
Event rate corrected for pion absorption.

FIG. 1. INELASTIC EVENTS											
	1963	1964	Total	$N_p=0$	$\frac{N_p=0}{N_n \geq 1}$	$N_p=1$	$N_n > 1$	$M^x < 1.4$	$M^x > 1.4$		
$1 \pi^+$	28	39	57	14	5	35	18	54	13		
$1 \pi^-$	2	3	5	0	0	1	4	3	2		
$m \gamma$ $m=1,2$	13	12	25	1	0	17	7	22	3		
no $\pi$ (el. rej.)	8	19	27	0	0	6	21	24	3		
$1 \pi^+ nC$	4	8 (1)	12 (1)	}	0	7	5	5	7		
$1 \pi^- nC$	3 (2) <sup>a)</sup>	4 (1)	7 (3)			0	7	1	6		
$m \gamma nC$ $m, n=1,2$	6	10 (3)	16 (3)			7	9	6	10		
Total $1 \pi$	64	95	159	15	5	73	71	115 <sup>*)</sup>	44		
$\pi^+ \pi^+$	1	1	2								
$\pi^+ \pi^0 nC$ <sup>c)</sup>	5 (3) <sup>b)</sup>	10 (3)	15 (6)								
$\pi^+ \pi^- nC$	4 (2)	10 (6)	14 (8)								
$\pi^0 \pi^0 nC$	1 (1)	2 (2)	3 (3)								
$\pi^- \pi^0 nC$	1	1 (1)	2 (1)								
$\pi^- \pi^-$	0	1	1								
Total $2 \pi$	12	25	37							10	27
Total $3 \pi-6 \pi$	16	25	41							3	38
Total Inel.	92	145	237							128	109
$m \pi nC$ ( $m \geq 3$ )											
X					Total charge of X						
	3	4	5	6	4+	3+	++	+	0	-	--
$m=x$	27	6	7	1	0	1	6	12	13	8	1
$m+n=x$	11	12	8	10	1	5	8	17	10	0	0
a) The numbers in parenthesis correspond to $n=2$ b) $0 \leq n \leq 2$ c) $n=0$											
*) number corrected for $1 \pi$ absorption 116											

FIG. 2.

EFFECTIVE MASS ALL MESONS IN EVENTS WITH  $E_{VIS} > 6.0$  GEV  
 MESON CHARGE +1.

14	EVENTS	ON HISTOGRAM	
2	EVENTS	UNMEASURABLE	
5	EVENTS	MESONIC CHARGE	+ 2
1	EVENTS	MESONIC CHARGE	- 1
1	EVENTS	MESONIC CHARGE	0

TOTAL 23

Note: ALL AMBIGUITIES RESOLVED  
 TO GIVE CHARGE +1

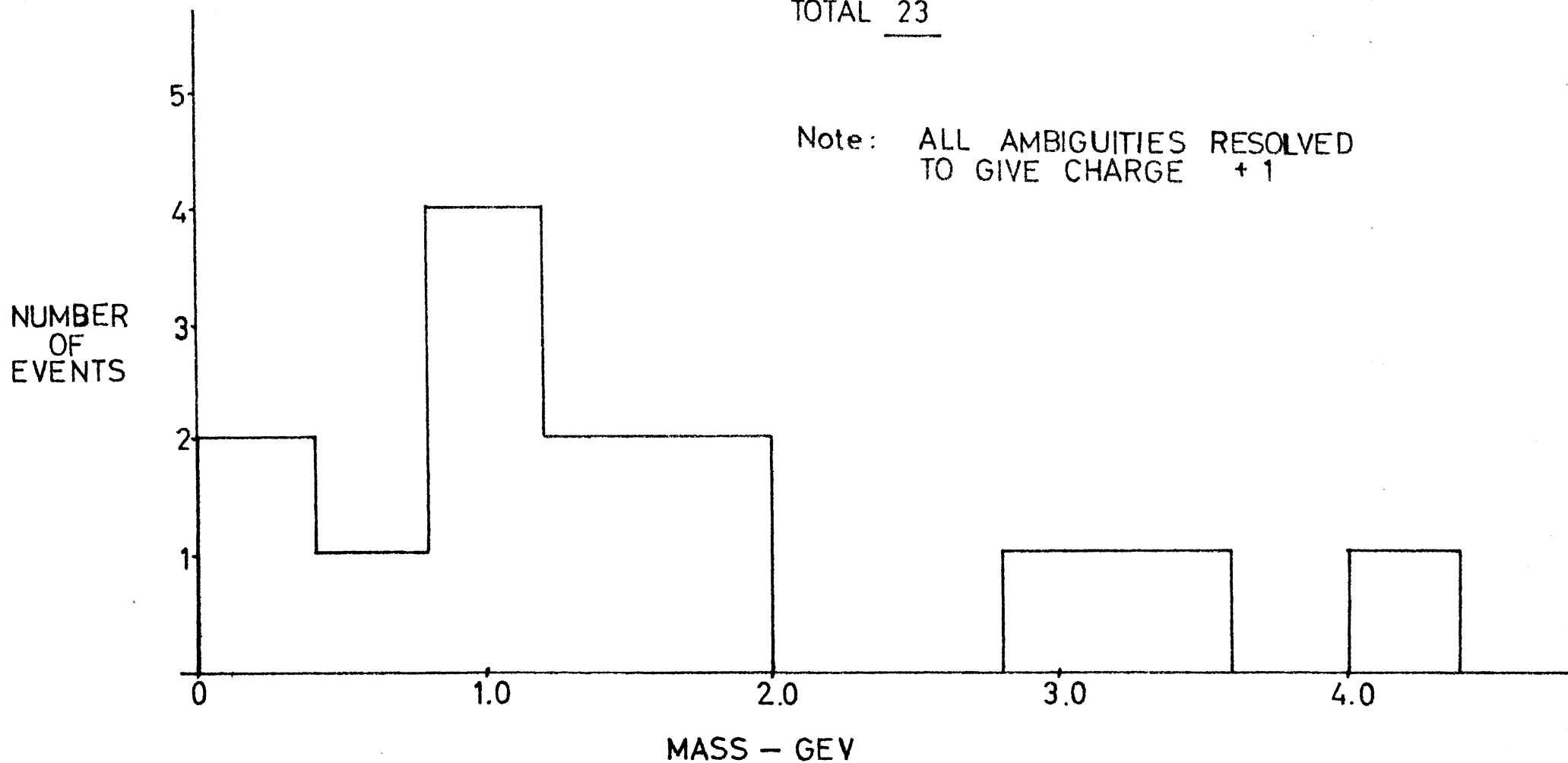




FIG. 3.

CORRECTED FOUR-MOMENTUM DISTRIBUTION  
FOR EVENTS WITH  $E_{vis} > 1$  Gev

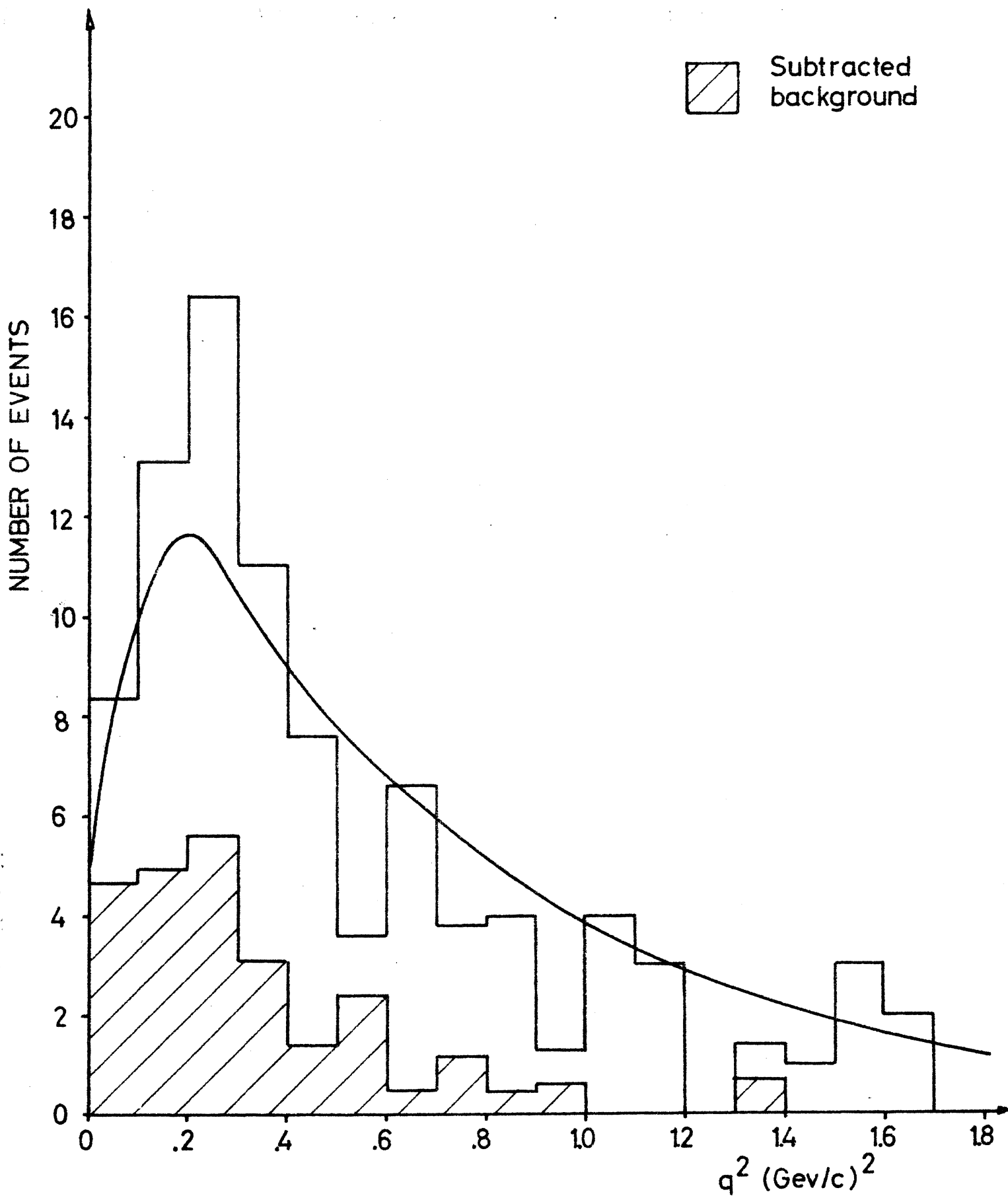


FIG. 4.

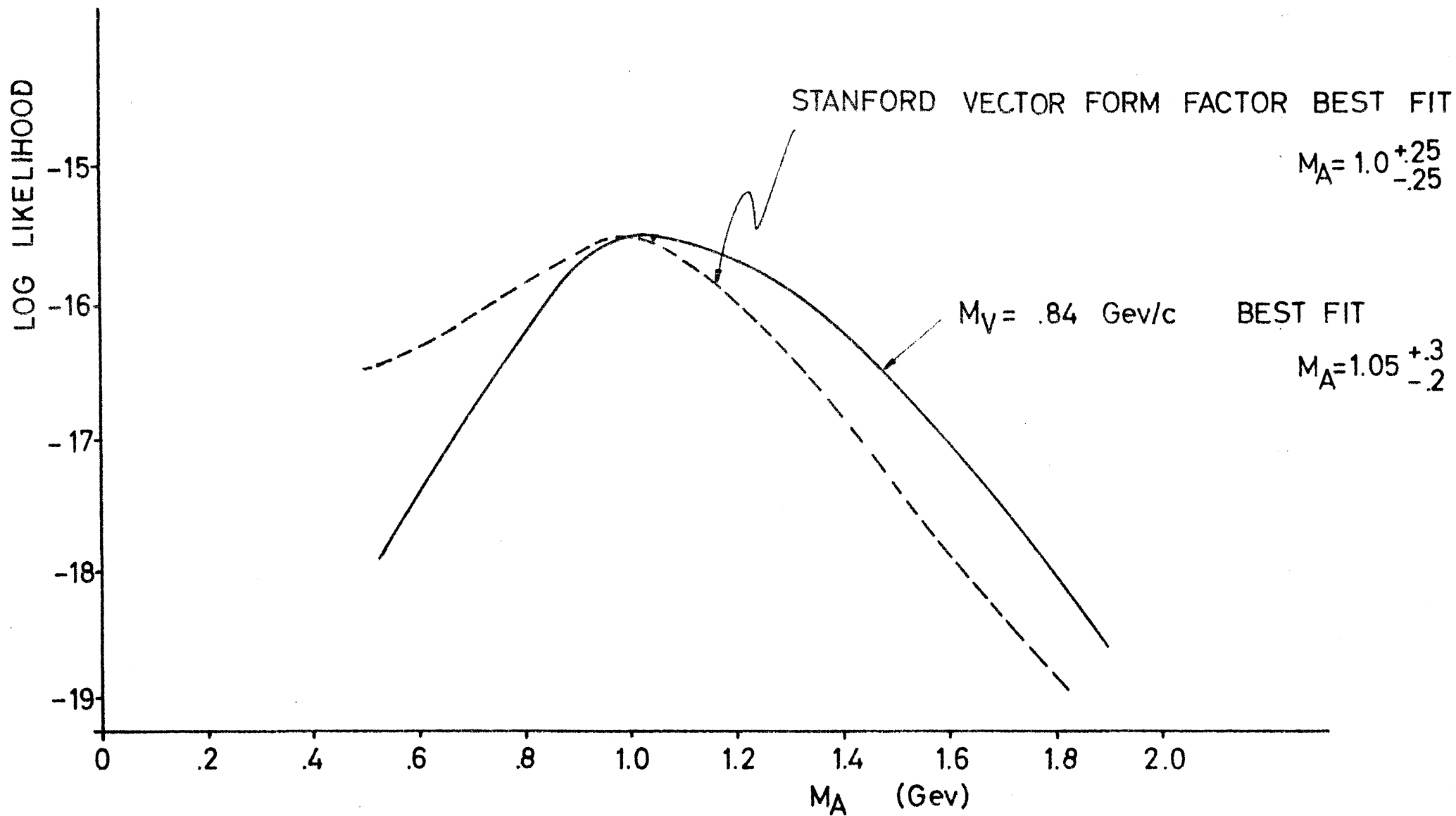


FIG. 5.

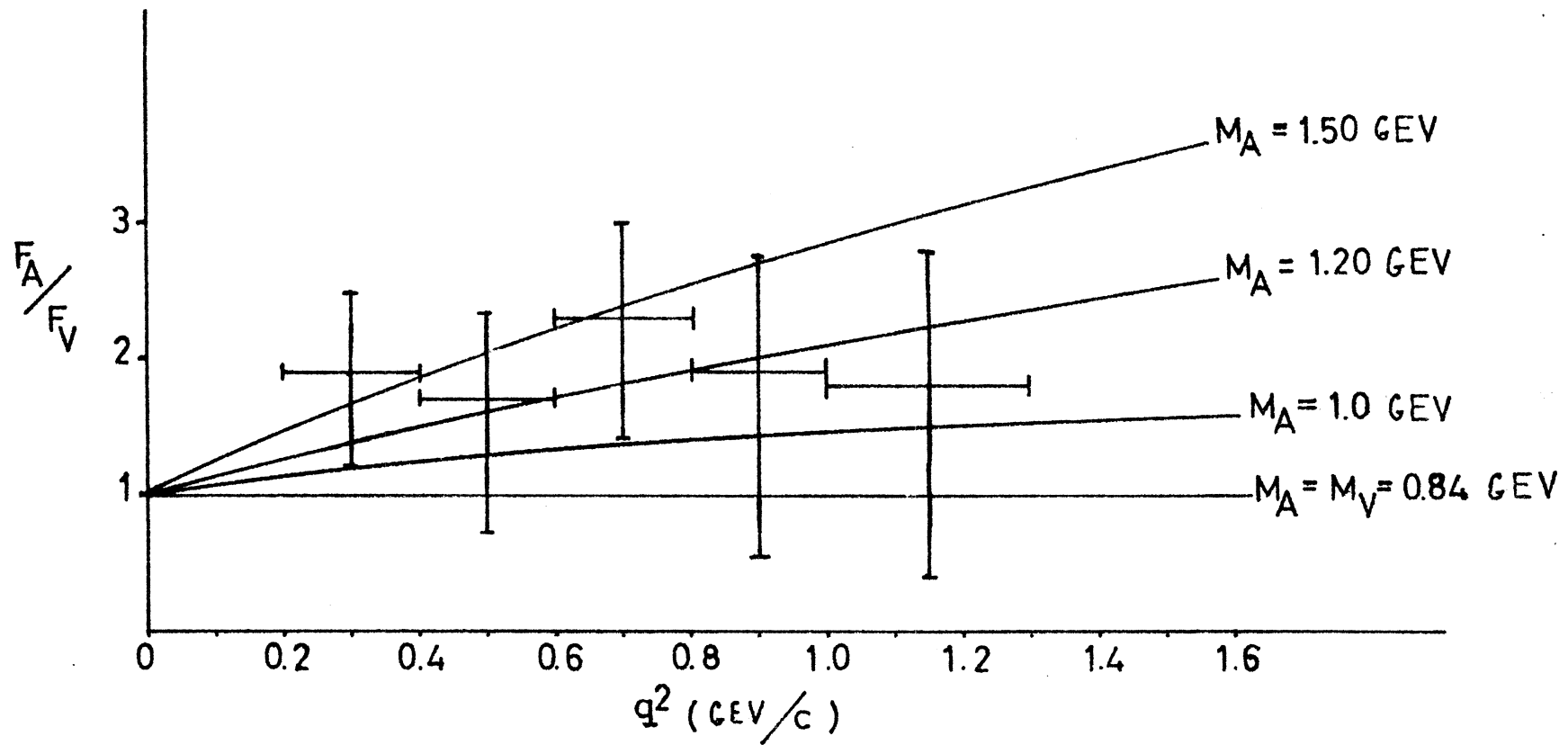
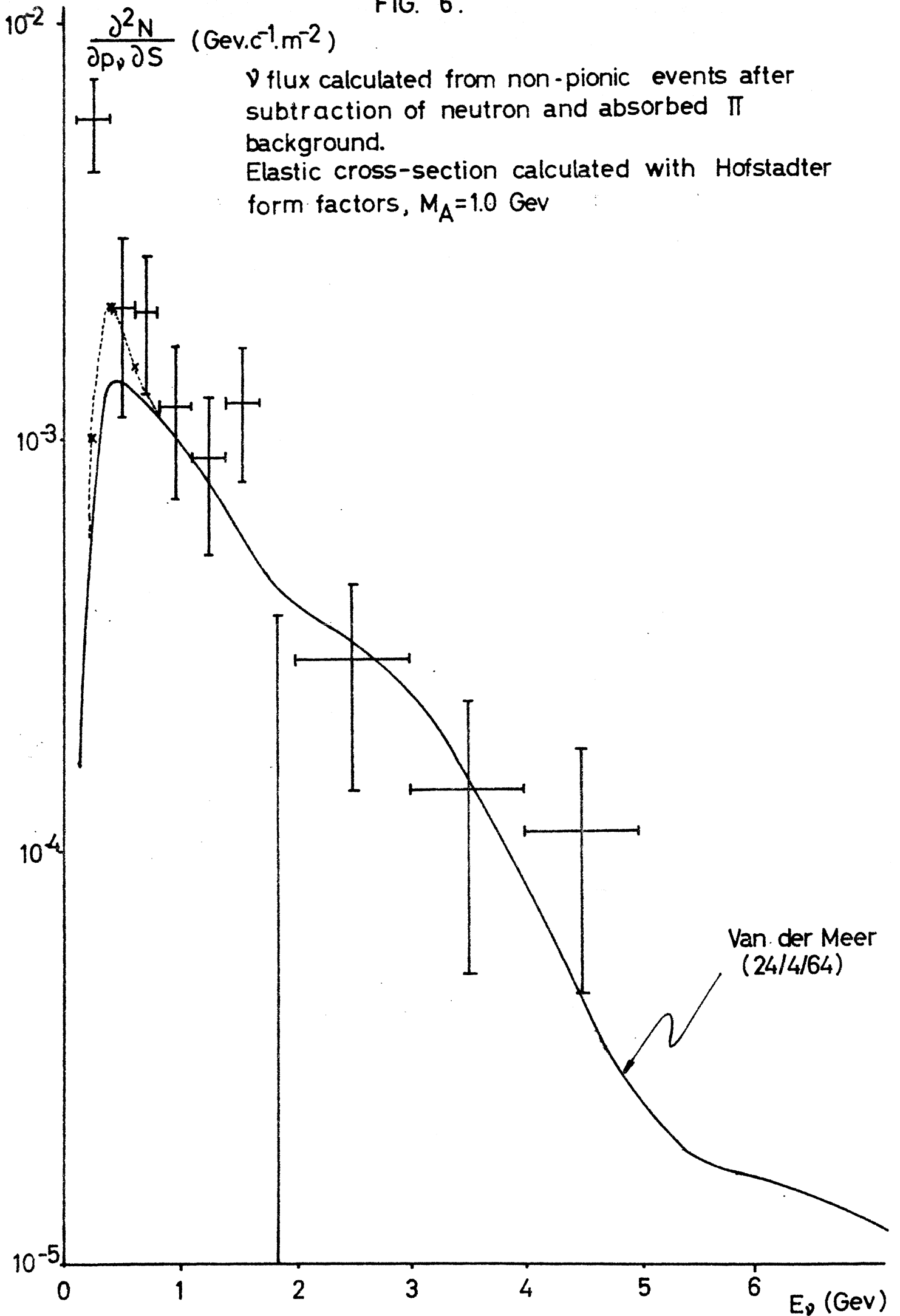


FIG. 6.



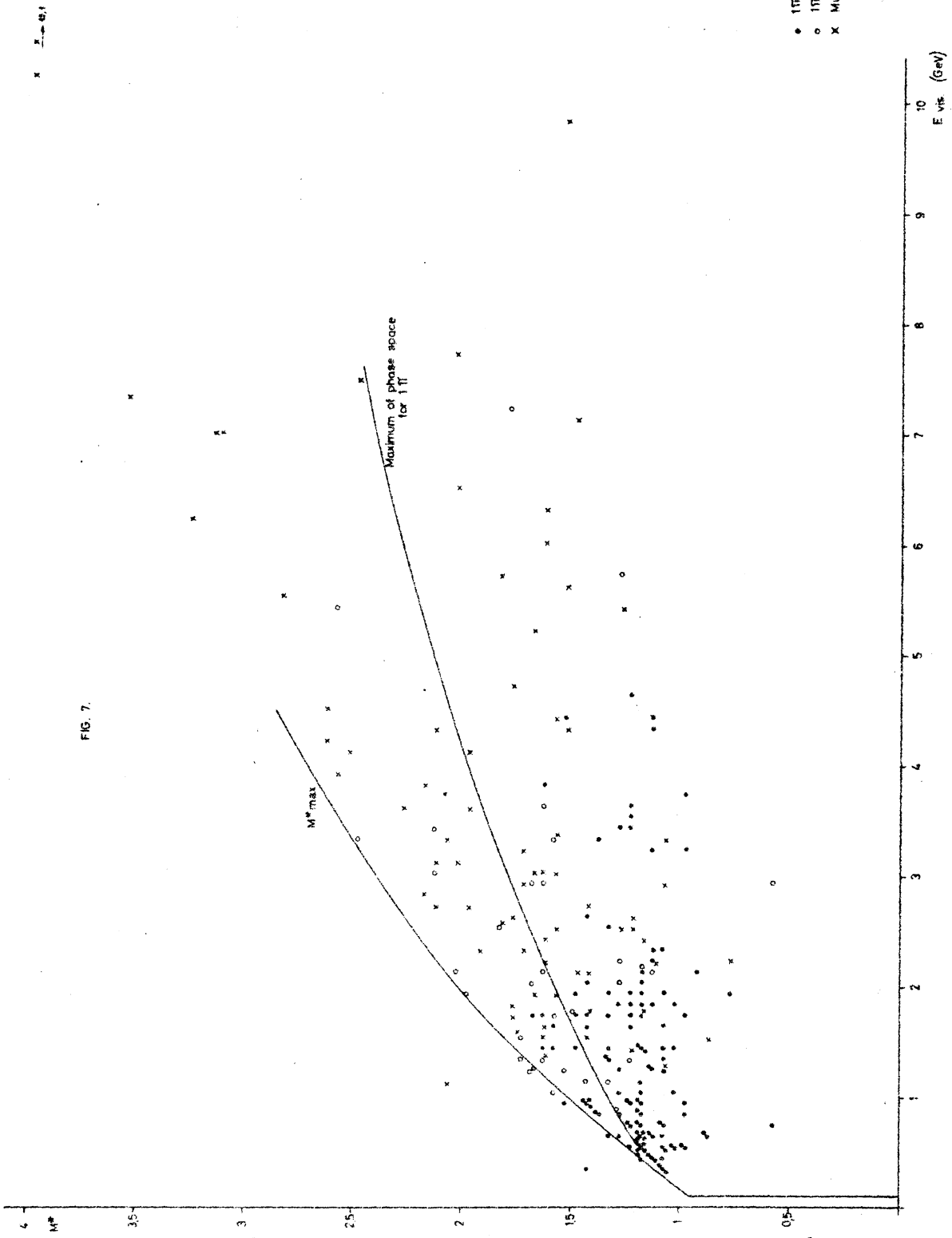
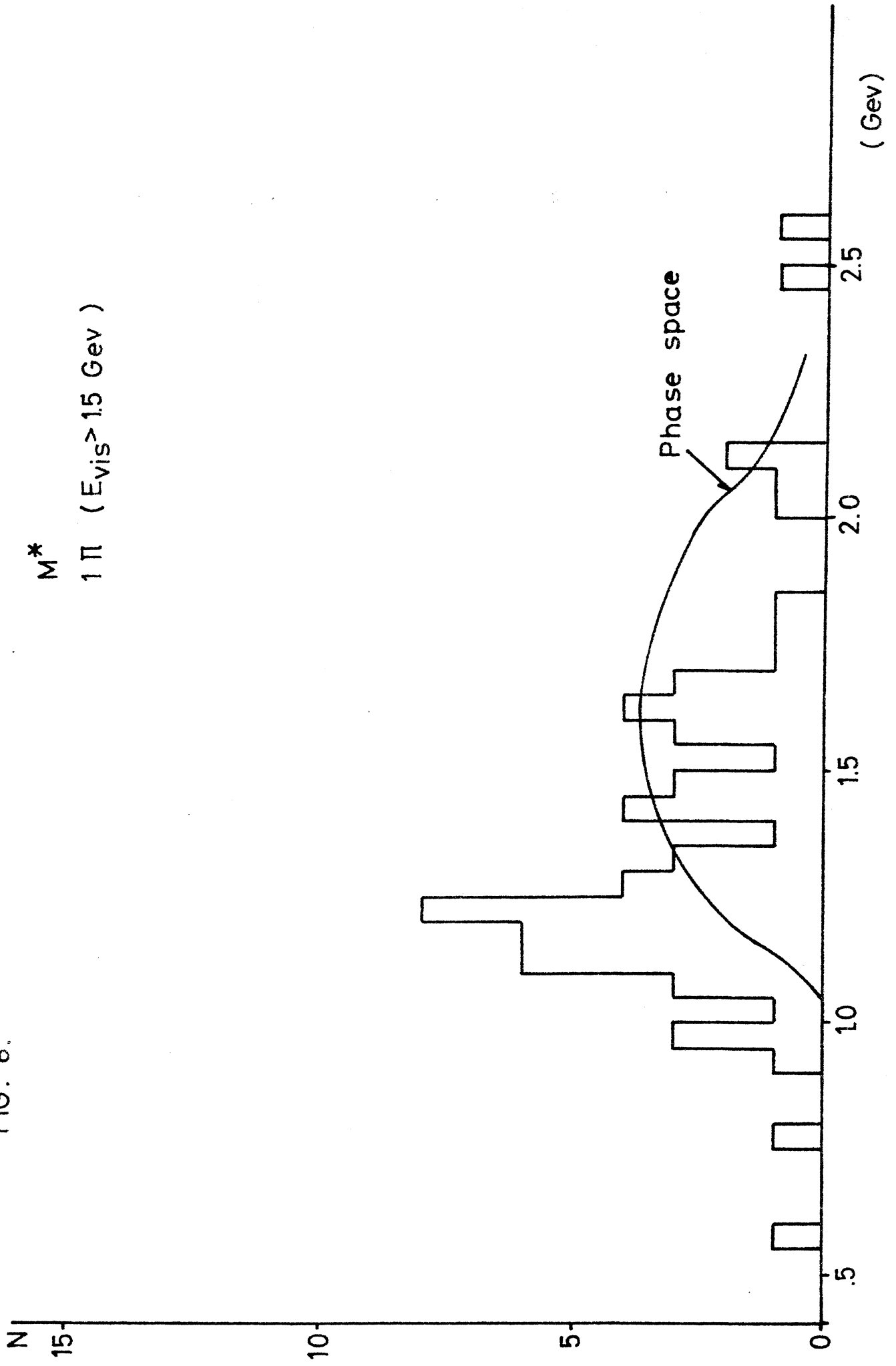


FIG. 7.

FIG. 8.



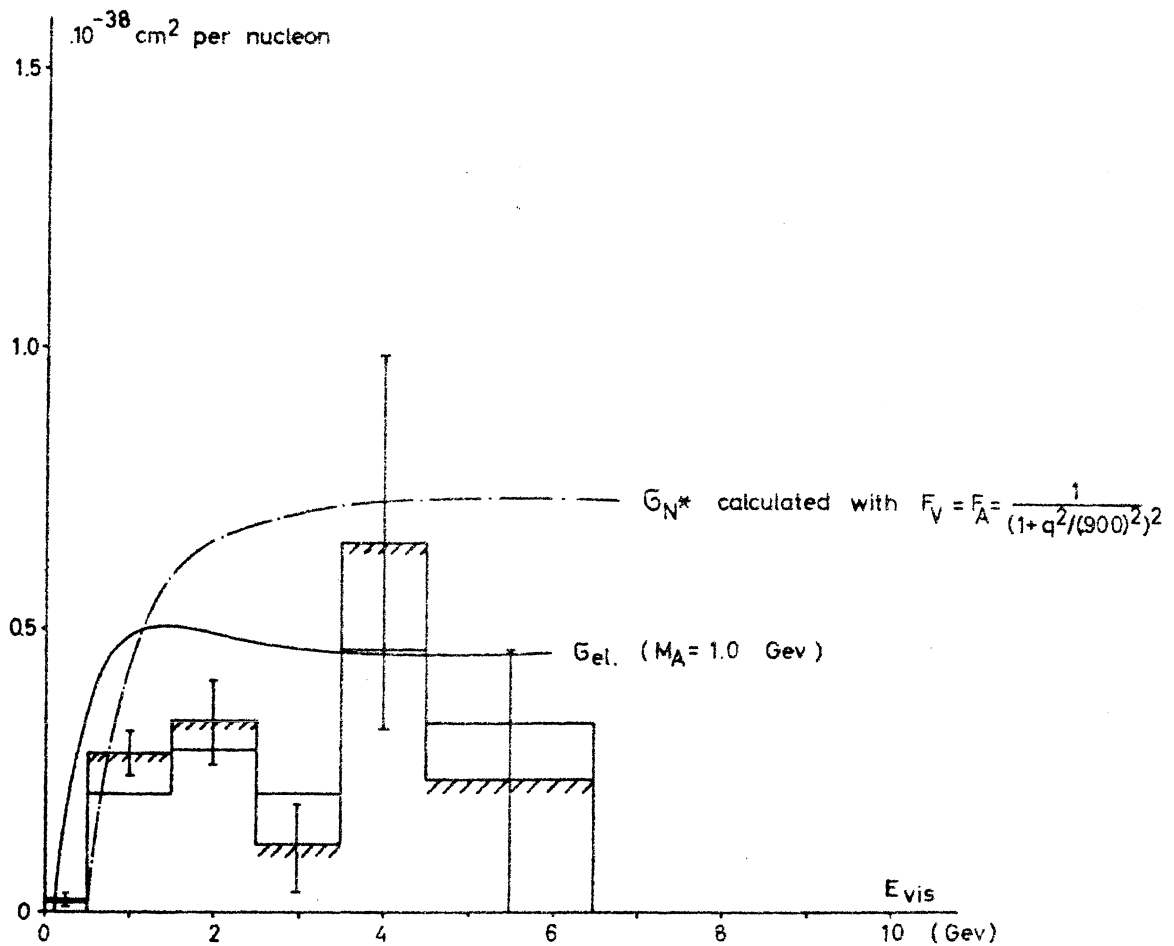
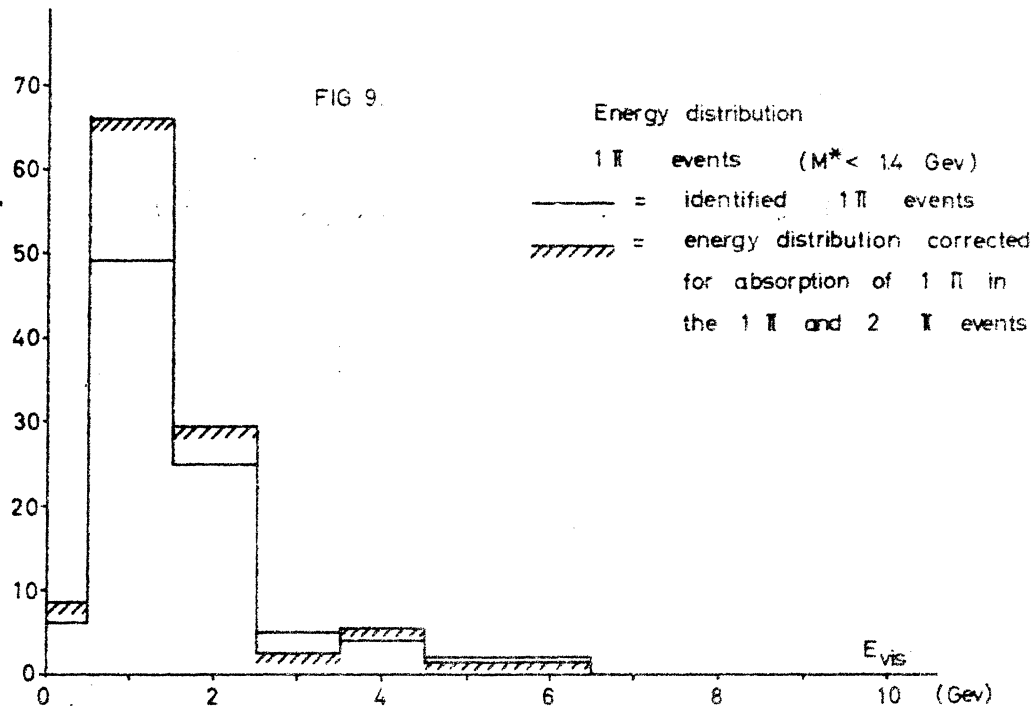


FIG. 10.

